Journal of
Manufacturing and Materials Processing

MDPI

Article

Effects of Oil Concentration in Flood Cooling on Cutting Force, Tool Wear and Surface Roughness in GTD-111 Nickel-Based Superalloy Slot Milling

Gábor Kónya * and Zsolt F. Kovács

Department of Innovative Vehicles and Materials, GAMF Faculty of Engineering and Computer Science, John von Neumann University, Izsáki St. 10, H-6000 Kecskemét, Hungary; kovacs.zsolt@nje.hu
* Correspondence: konya.gabor@nje.hu

Abstract: Cooling–lubricating processes have a big impact on cutting force, tool wear, and the quality of the machined surface, especially for hard-to-machine superalloys, so the choice of the right cooling–lubricating method is of great importance. Nickel-based superalloys are among the most difficult materials to machine due to their high hot strength, work hardening, and extremely low thermal conductivity. Previous research has shown that flood cooling results in the least tool wear and cutting force among different cooling–lubricating methods. Thus, the effects of the flood oil concentration (3%; 6%; 9%; 12%; and 15%) on the above-mentioned factors were investigated during the slot milling of the GTD-111 nickel-based superalloy. The cutting force was measured during machining with a Kistler three-component dynamometer, and then after cutting the tool wear and the surface roughness on the bottom surface of the milled slots were measured with a confocal microscope and tactile roughness tester. The results show that at a 12% oil concentration, the tool load and tool wear are the lowest; even at an oil concentration of 15%, a slight increase is observed in both factors. Essentially, a higher oil concentration reduces friction between the tool and the workpiece contact surface, resulting in reduced tool wear and cutting force. Furthermore, due to less friction, the heat generation in the cutting zone is also reduced, resulting in a lower heat load on the tool, which increases tool life. It is interesting to note that the 6% oil concentration had the highest cutting force and tool wear, and strong vibration was heard during machining, which is also reflected in the force signal. The change in oil concentration did not effect the surface roughness.

Keywords: nickel-based superalloys; flood cooling; oil concentration; tool wear; surface roughness

Citation: Kónya, G.; Kovács, Z.F. Effects of Oil Concentration in Flood Cooling on Cutting Force, Tool Wear and Surface Roughness in GTD-111 Nickel-Based Superalloy Slot Milling. *J. Manuf. Mater. Process.* **2024**, *8*, 119. https://doi.org/10.3390/jmmp8030119

Academic Editor: Steven Y. Liang

Received: 14 May 2024
Revised: 1 June 2024
Accepted: 6 June 2024
Published: 7 June 2024

1. Introduction

Nickel-based superalloys are highly challenging to machine because of their elevated tensile strength and hardness at high temperatures, coupled with poor thermal conductivity and low elongation at break [1–5]. These mechanical and physical properties reduce the machinability of these materials [6]. High thermal load (at 1000 °C) and substantial tool loading occur during the machining process, leading to significant cutting forces and vibrations [3,7]. Consequently, this results in rapid wear of cutting tools and frequent tool breakages [8,9]. Tool wear is a complex occurrence stemming from the interaction of mechanical (abrasion) and chemical (diffusion) factors between the cutting tool and the workpiece during machining procedures. When machining nickel-based superalloys, different types of tool wear—like mechanical wear, adhesive wear, diffusion wear, and oxidation wear—become notably more pronounced and challenging [10–12]. Furthermore, extremely precise tolerances must be maintained concerning the components' geometry, a factor significantly influenced by tool wear [13–15]. The presence of a substantial amount of metal carbides (MC, $M_{23}C_6$) in the raw material further exacerbates tool wear [16]. Owing to these characteristics, achieving high technological parameters is not feasible using metal carbide cutting tools, unlike ceramic tools that are capable of attaining cutting speeds of up to 1000 m/min [17,18].

Machinability is influenced by several factors such as material properties, system characteristics, and various cutting parameters and settings, as shown in Figure 1. These factors act as a system to influence tool wear, tool life and load, size and shape accuracy, and surface roughness of the machined surface [16,19–21]. Of these factors, the effects of cooling–lubricating processes will now be addressed.

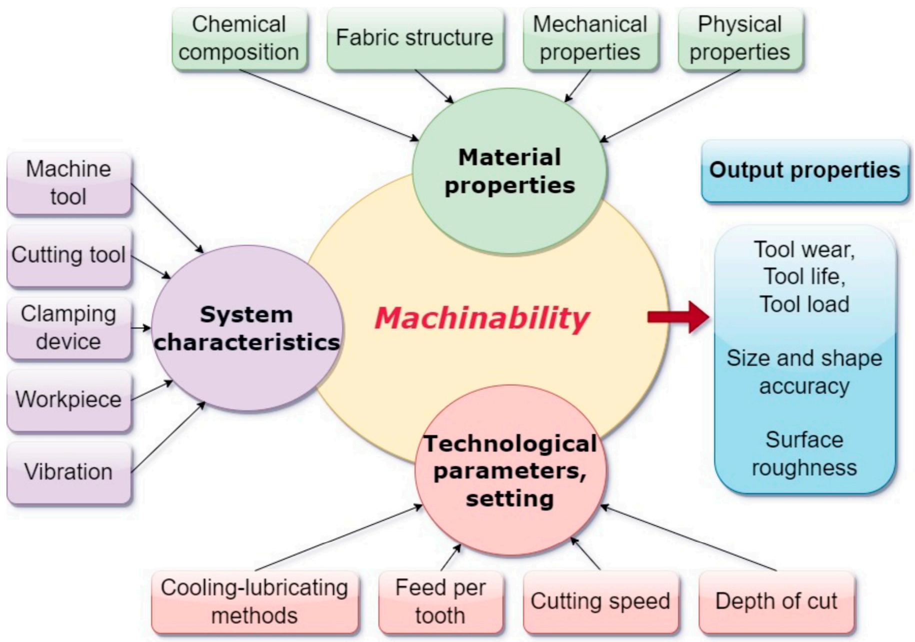

Figure 1. Factors affecting machinability.

During chip removal, three distinct zones emerge at the contact of the tool and workpiece surfaces. These are the primary shear zone (PSZ), characterized by the rapid shearing of metal volumes transitioning from the workpiece material into the forming chip; the secondary shear zone (SSZ), which forms due to friction at the tool–chip interface; and the tertiary shear zone (TSZ), where plastic deformation occurs because of the interaction between the newly machined surface of the workpiece and the tool flank [22]. In these zones, intense friction leads to the generation of high temperatures and extremely elevated local loads [23]. In the machining of various nickel-based superalloys, several cooling–lubricating or heating processes such as flood [1,24], MQL (minimum quantity lubrication) [25,26], cryogenic cooling with LCO_2 (liquid carbon dioxide) [27] and LN_2 (liquid nitrogen) [28], the combination of cryogenic cooling and MQL (CryoMQL) [29], LAM (laser-assisted machining) [30,31], and gas flame [32,33] and induction-assisted [34,35] heating are used to reduce friction and thus increase tool life, reduce the amount of cutting force and energy consumption, and improve the surface quality of the machined part [36,37]. Cooling techniques are essential in machining superalloys. Although applying cutting fluid to the machining zone is complex, it offers significant benefits by providing effective lubrication and cooling. Machining superalloys without coolant is nearly impossible due to their material properties. The high temperatures generated during machining cause the tool to anneal and wear, while the material's high thermal strength and work hardening lead to high cutting forces. The only way to reduce this phenomenon is to use cutting fluid [38–40]. Numerous studies [26,41,42] have shown that machining these materials whilst dry does not work with carbide tools. This is because dry machining lacks a cooling and lubricating medium to dissipate the high cutting temperatures from the zone and to lubricate the contact surface between the tool and the workpiece. When machining with emulsion and MQL cooling, the cutting force was nearly halved, and wear was significantly reduced compared to dry machining.

The oldest cooling–lubrication method is traditional flood cooling, which significantly enhances machining performance due to its lubrication, cooling, and chip removal functions. It also reduces the adhesion on the contact surfaces between the tool and the workpiece, thereby decreasing the cutting force during machining [43,44]. It also improves the surface quality of the component and provide corrosion resistance [45,46]. Cutting fluids can be classified into three main groups: oil-based, gas-based, and water-based. Of these, water-based cutting fluids are most commonly used when machining difficult-to-machine alloys. They can be solution- or emulsion-based, using synthetic or semi-synthetic oil [47]. These water-based cutting fluids provide favorable conditions for bacterial colonization. The fumes and suspended particles generated during their use can cause respiratory and other health problems [48,49]. Furthermore, when released into the environment, they result in severe environmental toxicity, which is why strict regulations govern how and under what conditions these cutting fluids can be used and how they must be disposed of. To avoid or mitigate this, there is a growing demand among manufacturers for vegetable oils, which are biodegradable and offer good performance in terms of cost-effectiveness compared to synthetic cutting oils [50]. Nevertheless, emulsified flood cooling has yet to become truly environmentally friendly, as it consumes many natural resources, and its disposal is also polluting [51–53]. Therefore, researchers have begun to explore new, more environmentally friendly cooling and lubrication methods.

Innovative technologies such as MQL, cryogenic cooling, and, later, the combination of cryogenic cooling and MQL for machining processes have emerged in the field of cooling and lubrication. The MQL technique is also referred to as near-dry lubrication, micro lubrication, and near-dry machining [54,55], where the lubrication flow rate in machining is between 10 and 100 mL/h [56]. This amount of oil, sprayed with air in droplets, is sufficient to form a thin oil film between the contact surfaces of the tool and the workpiece, reducing the friction and heat generation coefficients [57]. Cryogenic cooling is extremely beneficial in keeping the cutting temperature low during machining, which helps to prevent the tool from reaching a softening temperature. To achieve even lower temperatures, liquid nitrogen is used as a coolant, as it has a boiling point of −197 °C [28]. This advantage is usually complemented by MQL, in which a mixture of oil particles and air is injected into the cutting zone to reduce friction between the cutting tool and the machined surface [1,25,27]. These cooling–lubricating methods are significantly more environmentally friendly compared to flood cooling [58].

From a technological perspective, however, flood cooling still plays a significant role in the machining of difficult-to-cut alloys, especially when using conventional technological parameters. Patel et al. [24] turned 30 mm diameter, hot-rolled Nimonic 90 material using Kyocera-made coated 120408MS-PR1535 tungsten carbide inserts under various technological parameters and with both wet and liquid carbon dioxide cooling. The results show that in all cases, the cutting force was approximately 30% higher with liquid carbon dioxide cooling than with wet cooling. This is due to strain hardening occurring at low temperatures. However, tool wear was significantly lower with LCO_2 cooling compared to wet cooling. This difference is particularly noticeable at higher technological parameters. At lower technological parameters, this difference in wear decreases. The average surface roughness was higher in all cases with LCO_2 cooling compared to wet cooling. This can be attributed to the lack of lubrication between the tool and the workpiece contact surface. Pereira et al. [27] milled an Inconel 718 nickel-based superalloy using an S10 carbide end mill with TiAlN coating under constant technological parameters in wet, MQL, externally and internally applied CO_2, and CryoMQL environments. Regarding cutting forces, no significant difference was observed, although the lowest forces were recorded with wet cooling. However, the tool life was three times longer with wet cooling compared to externally applied CO_2 cooling. In wet machining, only adhesion was observed on the tool edge, whereas in other cases, this was accompanied by edge chipping as well.

Kaynak et al. [59] machined a hot-rolled Ti-5Al-5V-5Mo-3Cr titanium alloy using uncoated 883 grade inserts under various technological parameters in MQL, flood cooling, and high-pressure coolant (HPC) environments. They found that tool wear generally increased with the cutting speed; however, the rate of increase was significantly smaller with flood cooling and HPC compared to MQL. No significant difference in cutting force was observed in the lower cutting forces, but at a cutting speed of v_c = 210 m/min, the cutting force was significantly reduced with HPC.

Kónya and Kovács stated in their research [1,60] that when milling GTD-111 nickel-based superalloys, cryogenic cooling is not beneficial to the tool life, as high wear and chipping are observed at the tool edge; even with flood cooling, only minimal wear is observed. In addition, the surface roughness also deteriorated significantly at the bottom of the slot. Only chip breakage improved, as the material became brittle due to the cryogenic cooling. These results were greatly improved by the use of cryogenic cooling with liquid CO_2 and minimum quantity lubrication (MQL) since, in addition to cooling, lubrication is also present. Overall, the results show that lubrication has a greater effect on tool life than cooling. Since cryogenic cooling did not improve the tool life, tool loading, and surface roughness of the machined surfaces of GTD-111 nickel-base superalloys, the aim of this paper is to investigate the effects of oil concentration of flood cooling and find the most favorable one for the cutting force, tool wear, and surface roughness of the bottom of the milled slot.

2. Materials and Methods

2.1. Experimental Procedure

The experimental procedure is illustrated in Figure 2. In the experiments, the impacts of the oil concentration of the flood on the cutting force, tool wear, and surface roughness at the bottom of the milled slots were investigated. MOL Emolin 120-type biostable oil was used. The concentrations were adjusted with a Blaser-type refractometer, Blaser.swisslube; Distributor: Helvet Kft.; Distributor's city and country: Pilisvörösvár, Hungary. The experimental parameters are shown in Table 1. For slot milling, a BZL5D080R10L064S18P-type TiALN coated carbide end mill was used. It had a diameter of 8 mm, 5 cutting edges, and a corner radius of 1 mm. The axial depth of cut was initially a_p = 8 mm; then, due to tool breakage at low oil concentration, it was reduced to a_p = 4 mm. The size of the milled slots was 40 × 8 × 4 mm. Hard milling involves high levels of stress on a machine tool, demanding a robust and exceptionally rigid machine; therefore, the NCT-EmL 850D was chosen for the experiment. For the cutting force measurement, a KISTLER 9257B-type dynamometer with a KISTLER 5007-type charge amplifier unit was utilized. The measured force signals were recorded with Dynoware software Version 3.2.5.0 and evaluated in OriginPro 2021 software.

An Olympus LEXT OLS5000 confocal laser scanning measuring microscope was used to measure tool wear. The field view was 2600 × 2600 µm; the magnification was 1×. Each cutting edge of the 5-edged tool was measured 3 times, and the average flank wear (VB) and the dispersion were determined. For measuring the average surface roughness (R_a) and main roughness depth (R_z), a Mitutoyo Formtracer SV-C3100 tactile roughness tester was utilized. Each milled slot was measured 3 times, and the results were evaluated in Microsoft Excel.

Table 1. Experimental parameters for slot milling.

Cutting Speed v_c (m/min)	Feed per Tooth f_z (mm/tooth)	Depth of Cut a_p (mm)	Oil Concentration (wt. %)
21	0.01	firstly, 8 mm after breaking after the whole experiment, 4 mm	3; 6; 9; 12; 15

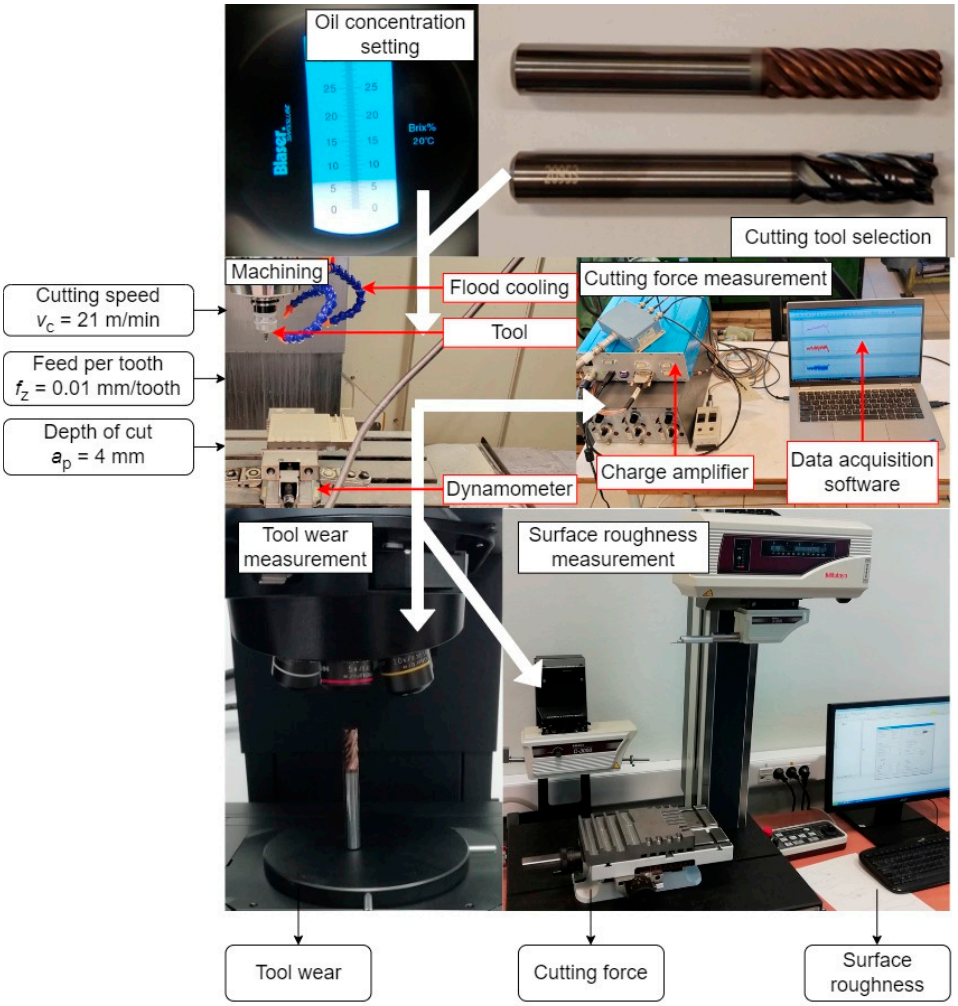

Figure 2. Experimental procedure.

2.2. Material

In the experiments, the GTD-111 nickel-based superalloy was machined, the chemical composition and mechanical and physical properties of which are shown in Tables 2–4.

Table 2. Chemical composition of GTD-111.

Ni (wt. %)	C (wt. %)	Cr (wt. %)	Co (wt. %)	Al (wt. %)	Ti (wt. %)	W (wt. %)	Mo (wt. %)	Ta (wt. %)	B (wt. %)
62.37	0.06	13.7	9.0	2.8	4.7	3.5	1.4	2.4	0.05

Table 3. Mechanical properties of GTD-111.

Tensile Strength R_m (MPa)	Stretch A_5 (%)	Contraction Z (%)	Hardness HRC
1310	8	5	41.4

Table 4. Physical properties of GTD-111.

Density ρ (kg/m^3)	Thermal Conductivity at 20 °C λ (W/m·K)	Specific Heat at 20 °C c (J/kg·K)
8000	12.56	0.452×10^3

3. Results

3.1. Cutting Force

The evolution of the cutting force components and the calculated cutting force as a function of the machining time for an axial depth of cut of 8 mm are shown in Figure 3. It can be seen that at the 3% oil concentration, the x and y directions of the cutting force immediately increased up to the 5000 N limit, and then broke after nearly 30 s, after a machined length of about 20 mm, as shown in Figure 4. At 6% oil concentration, the force rise was less steep than at 3%, but the load reached the measurement limit and broke at 42 s, which represents a machined length of 26 mm. Tool failure occurred in both oil concentration cases, starting with the chipping of the corners; then, the edges chipped, and finally, the tool body fractured. This can be attributed to insufficient lubrication, which failed to compensate for the friction generated on the contact surface of the tool and workpiece due to the large depth of cut, leading to heat buildup that softened the tool edge and initiated premature tool failure. As the tool broke at both oil concentrations, the axial depth of cut was reduced to 4 mm.

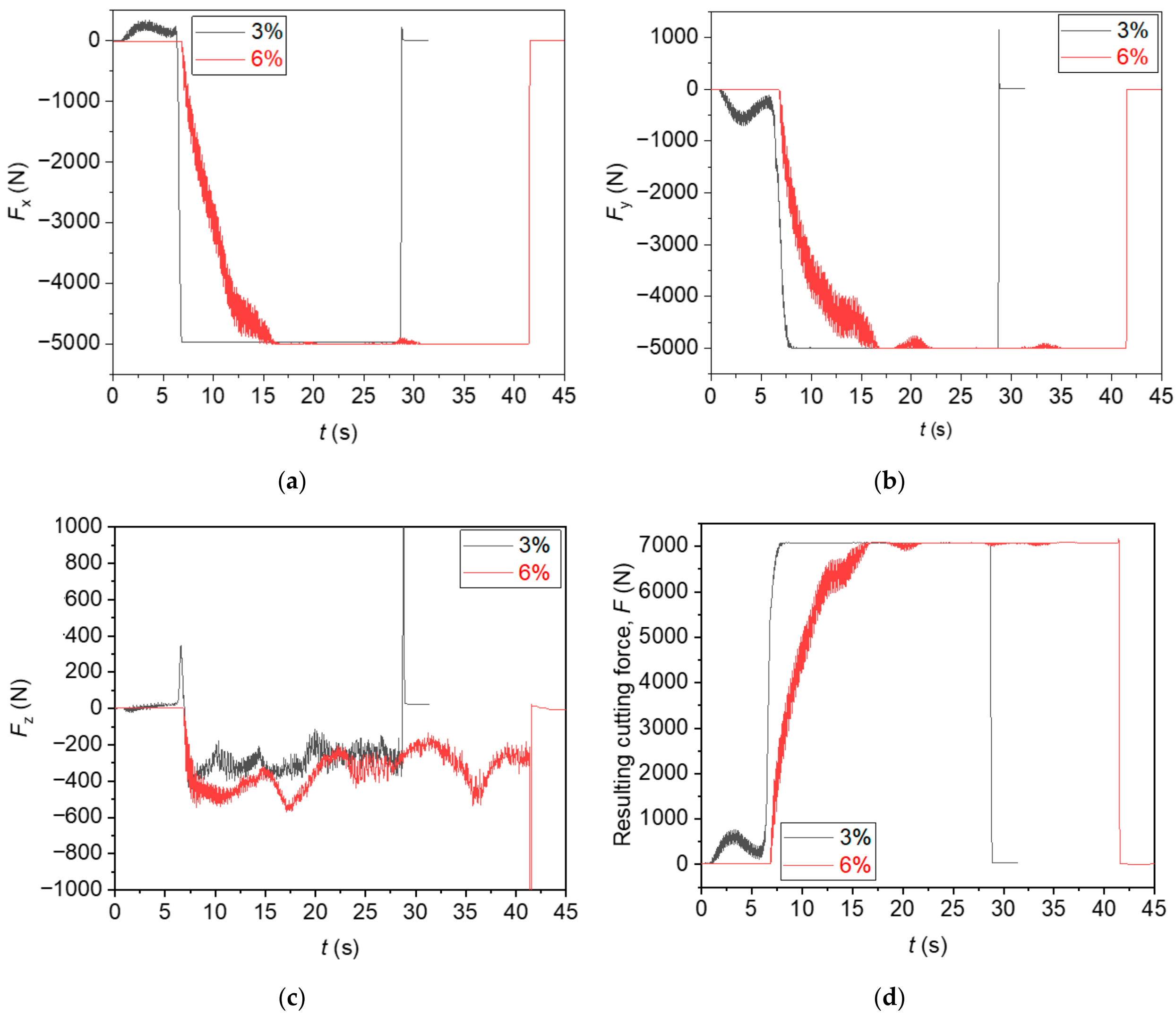

Figure 3. (**a**) F_x; (**b**) F_y; (**c**) F_z; and (**d**) F resulting cutting force as a function of machining time for an axial depth of cut of 8 mm.

Figure 4. Broken tool at 3% emulsion concentration.

The evolution of the cutting force components and the calculated cutting force as a function of the machining time for an axial depth of cut of 4 mm are shown in Figures 5 and 6. From the results, it can be seen that the highest cutting force was obtained at an oil concentration of 6%, and the highest vibrations were also obtained in this case, which can also be seen in the tool wear results in Figures 7 and 8. The lowest cutting force occurred at an oil concentration of 12% and increased again at 15%, suggesting that the optimum oil concentration is 12%. This is because too high an oil concentration causes an oil coating to build up on the cutting edge, which increases the cutting-edge radius, as after a coating process. These results suggest that it is better to use a higher oil concentration, as the lubricating effect of the emulsion has a greater influence on the cutting force. However, an oil concentration of 6% is to be avoided, which is interesting because the industry does not go above this level to reduce costs.

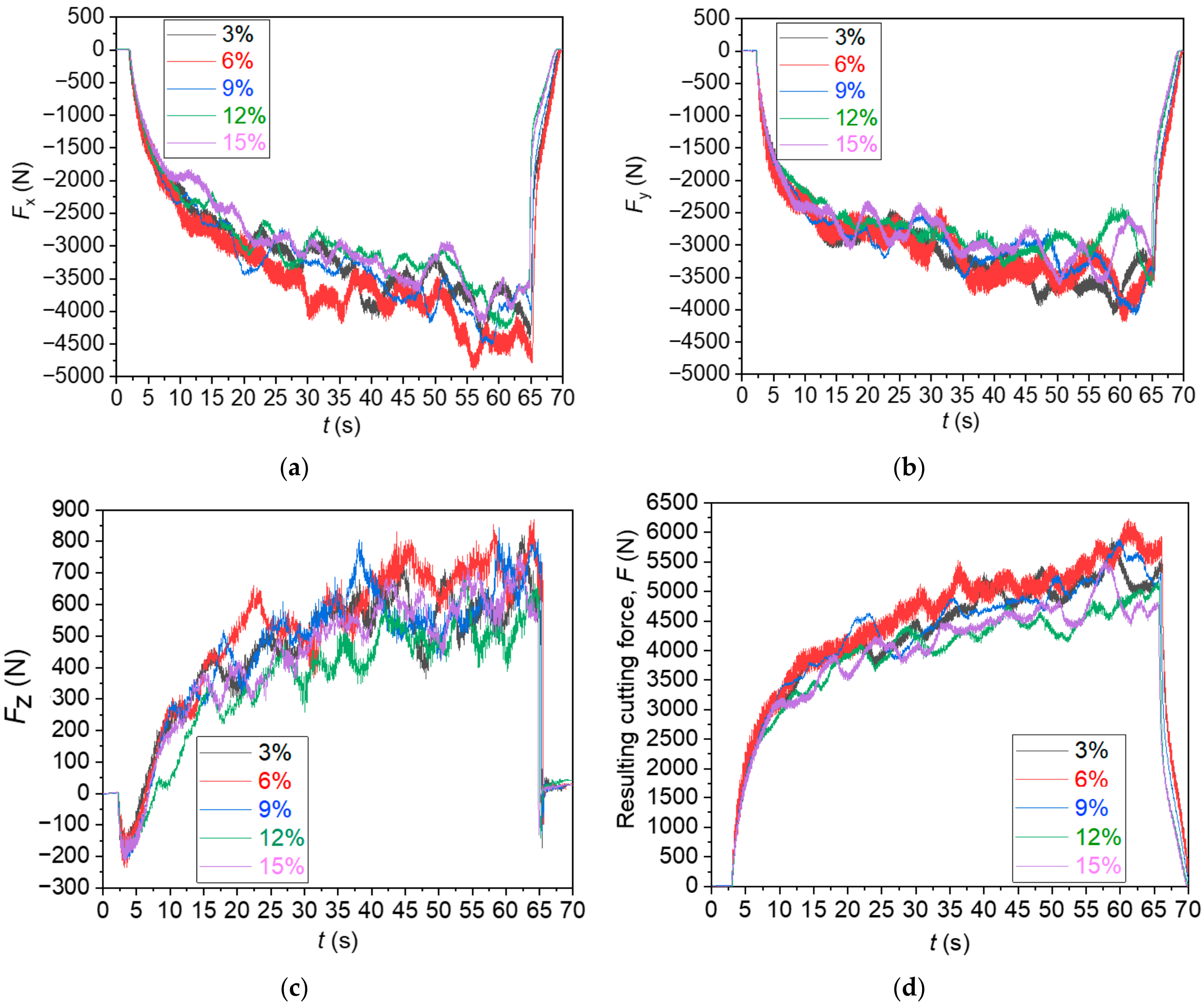

Figure 5. (**a**) F_x; (**b**) F_y; (**c**) F_z; and (**d**) resulting cutting force as a function machining time for an axial depth of cut of 4 mm.

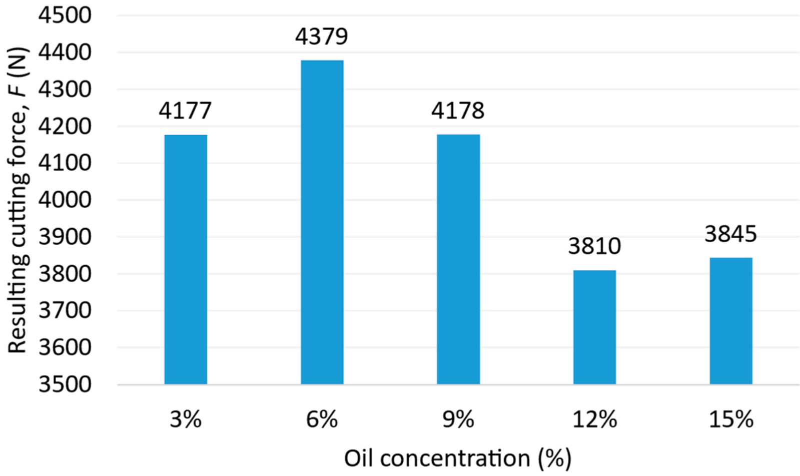

Figure 6. Main cutting force as a function of oil concentration.

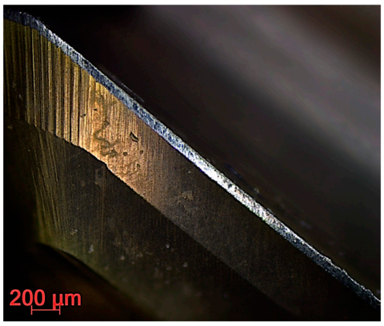

(**a**)

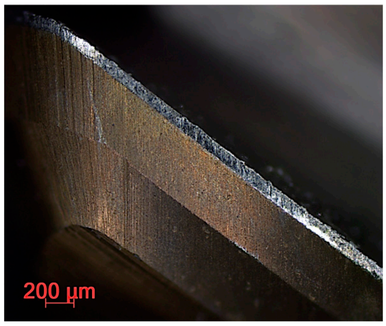

(**b**)

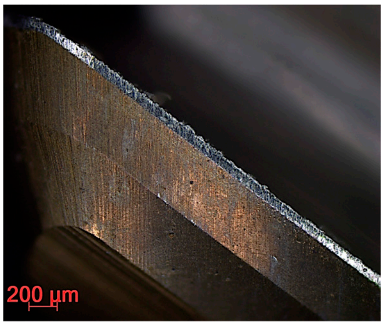

(**c**)

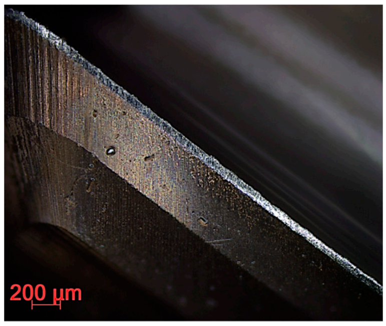

(**d**)

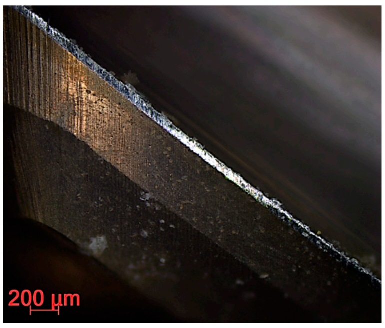

(**e**)

Figure 7. Microscopic images of the tools used at (**a**) 3%; (**b**) 6%; (**c**) 9%; (**d**) 12%; and (**e**) 15% oil concentrations.

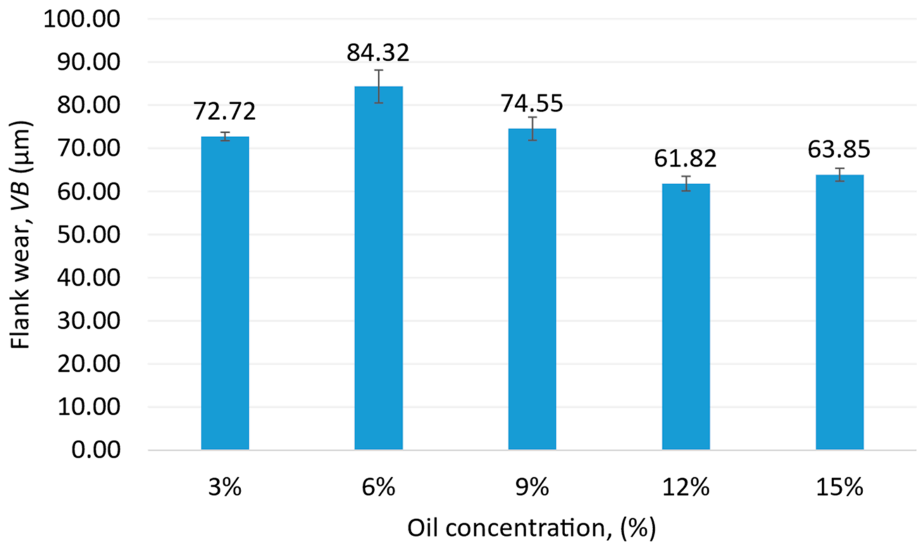

Figure 8. Tool wear as a function of oil concentration.

3.2. Tool Wear

Microscopic images of the tool are shown in Figure 7, and the results of the flank wear as a function of oil concentration are shown in Figure 8. For each of these oil concentrations, the edge in the worst condition is shown. The highest tool wear is observed at 6% oil concentration and the lowest at 12% oil concentration, which is related to the cutting forces. The dispersion of tool wear is also highest at 6% oil concentration. This is important because the dispersion is an indication of how even or how different the wear on the edges is. This large variance at 6% oil concentration indicates that one edge is more worn than the other edges, which is typically the first step in the failure phase of machining these materials. As one edge initially wears more, or possibly cracks, causing the chip cross-section removed by the edge to decrease, the next edge must remove more material, which means that the edge load will be higher, causing it to wear and break more. This process goes along all the edges of the tool. At oil concentrations of 3% and 6%, minimal cracking along the edge is also observed along with wear. Increasing the oil concentration fundamentally reduces tool wear, as in water-based emulsion, there is more oil; thus, it can lubricate the contact surface of the workpiece and tool more effectively, resulting in a decrease in the abrasive effect of the metal carbides found in the material, since the surfaces can slide against each other. Furthermore, friction also decreases, resulting in lower heat generation in the machining zone, and thus the tool will be subjected to less heat load.

3.3. Surface Roughness

The average surface roughness (R_a) and main roughness depth (R_z) as a function of the oil concentration in flood cooling are illustrated in Figure 9. The results show that the oil concentration content of the flood cooling has no significant effect on the surface roughness. The surface roughness is mainly influenced by the different cooling–lubricating processes, process parameters, and tool geometry [1,61]. If surface modification or better surface roughness is required, it can be achieved with unconventional technologies such as Electrical Discharge Machining (EDM) [62].

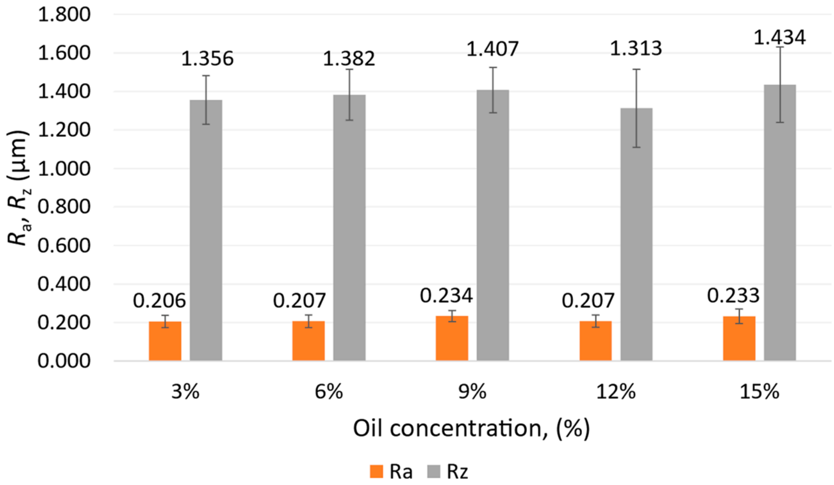

Figure 9. Average surface roughness (R_a) and main roughness depth (R_z) as a function of the oil concentration.

4. Conclusions

This paper investigated the effect of the oil concentration of the flood cooling on the output parameters such as cutting force, tool wear, and surface roughness of the milled slots. The authors state the following conclusions:

- The lowest cutting force at a 12% oil concentration of flood cooling, and the highest at the oil concentration of 6%, was observed. With the same noise filtering method, the highest fluctuation in the force signal is observed at 6% oil concentration, which is due to the higher vibration during machining.
- Consistent with the trend in cutting force, the lowest wear was measured at an oil concentration of 12%, and the highest at 6%. Vibrations during machining have a negative impact on both tool wear and tool life.
- The dispersion of the wear of five tool edges was calculated for an emulsion concentration of 6%, which shows that in this case, the wear of the edges was the most uneven, which accelerates the failure.
- The surface roughness is not influenced by the oil concentration content of the flood cooling; it is influenced by the cutting parameters and tool geometry.
- Increasing the oil concentration fundamentally decreases tool wear because in water-based emulsions, there is more oil available to lubricate the contact surface between the workpiece and the tool. This leads to a reduction in the abrasive effect of the metal carbides present in the material, as the surfaces can slide against each other more easily. Additionally, friction decreases, resulting in lower heat generation in the machining zone, thereby subjecting the tool to a reduced heat load. The choice of oil concentration has an even more significant effect at greater depth of cut, as shown in Figures 3 and 4.

Further research is aimed at examining the relationship between the oil viscosity used in emulsion and the oil concentration during the milling of nickel-based superalloys.

Author Contributions: Investigation, G.K. and Z.F.K.; writing—original draft, G.K. All authors have read and agreed to the published version of the manuscript.

Funding: This research received no external funding.

Data Availability Statement: No new data were created or analyzed in this study. Data sharing is not applicable to this article.

Conflicts of Interest: The authors declare no conflict of interest.

References

1. Kónya, G.; Kovács, Z.F. The Comparison of Effects of Liquid Carbon Dioxide and Conventional Flood Cooling on the Machining Conditions During Milling of Nickel-based Superalloys. *Period. Polytech. Mech. Eng.* **2023**, *67*, 190–196. [CrossRef]
2. Kun, K.; Kodácsy, J.; Vaczkó, D.; Kovács, Z.F. Machinability of Ni-based Superalloys by Indexable End Mills. *Acta Mater. Transylvanica* **2019**, *2*, 49–54. [CrossRef]
3. Guimaraes, M.C.R.; Fogagnolo, J.B.; Paiva, J.M.; Veldhuis, S.; Diniz, A.E. The impact of the cutting parameters and tool condition on surface integrity when milling Inconel 625. *J. Mater. Res. Technol.* **2023**, *25*, 1944–1958. [CrossRef]
4. Halim, N.H.A.; Haron, C.H.C.; Ghani, J.A. Sustainable Machining of Hardenes Inconel 718: A Comparative Study. *Int. J. Precis. Eng. Manuf.* **2020**, *21*, 1375–1387. [CrossRef]
5. Ratnam, C.; Kumar, K.A.; Murthy, B.S.N.; Rao, K.V. An experimental study on boring of Inconel 718 and multi response optimization of machining parameters using Response Surface Methodology. *Mater. Today Proc.* **2018**, *5*, 27123–27129. [CrossRef]
6. Faraz, M.I.; Petru, J. Evaluation of Machining Variables on Machinability of Nickel Alloy Inconel 718 Using Coated Carbide Tools. *Machines* **2024**, *12*, 4. [CrossRef]
7. Özbek, O.; Saruhan, H. The effect of vibration and cutting zone temperature on surface roughness and tool wear in eco-friendly MQL turning of AISI D2. *J. Mater. Res. Technol.* **2020**, *9*, 2762–2772. [CrossRef]
8. Xue, K.; Chen, P.; Liu, W.; Zou, B.; Li, L.; Chen, W.; Wang, X.; Xu, Z. Geometric Structures for Sialon Ceramic Solid End Mills and Its Performance in High-Speed Milling of Nickel-Based Superalloys. *Coatings* **2023**, *13*, 1483. [CrossRef]
9. Zhang, J.; Du, J.; Li, B.; Su, G. Investigation on White Layer Formation in Dry High-Speed Milling of Nickel-Based Superalloy GH4169. *Machines* **2023**, *11*, 406. [CrossRef]
10. Bilgin, M.; Karabulut, Ş.; Karakoç, H.; Kayır, Y.; Sarıkaya, M. An experimental investigation on machining-induced surface/subsurface characteristics of nickel based Inc-718 alloy: A novel hybrid approach in milling process. *Tribol. Int.* **2024**, *191*, 109120. [CrossRef]
11. Grzesik, W.; Niesłony, P.; Habrat, W.; Sieniawski, J.; Laskowski, P. Investigation of tool wear in the turning of Inconel 718 superalloy in terms of process performance and productivity enhancement. *Tribol. Int.* **2018**, *118*, 337–346. [CrossRef]
12. Zhu, D.; Zhang, X.; Ding, H. Tool wear characteristics in machining of nickel-based superalloys. *Int. J. Mach. Tools Manuf.* **2013**, *64*, 60–77. [CrossRef]
13. Soriano Gonzalez, L.; Medina Aguirre, F.; Soo, S.L.; Hood, R.; Novovic, D. Influence of Size Effect in Milling of a Single-Crystal Nickel-Based Superalloy. *Micromachines* **2023**, *14*, 313. [CrossRef] [PubMed]
14. Ezugwu, E.O. Key improvements in the machining of difficult-to-cut aerospace superalloys. *Int. J. Mach. Tools Manuf.* **2005**, *45*, 1353–1367. [CrossRef]
15. Molaiekiya, F.; Aliakbari Khoei, A.; Aramesh, M.; Veldhuis, S.C. Machined surface integrity of inconel 718 in high-speed dry milling using SiAlON ceramic tools. *Int. J. Adv. Manuf. Technol.* **2021**, *112*, 1941–1950. [CrossRef]
16. Singh, A.; Ghosh, S.; Aravindan, S. State of art for sustainable machining of nickel-based alloys using coated and uncoated tools and machining of high strength materials using surface modified cutting tools. *Tribol. Int.* **2022**, *170*, 107517. [CrossRef]
17. Kónya, G.; Szabó, N.; Kovács, Z.F. Investigation of the Machinability of GTD-111 Type Nickel-Base Superalloy During Face Milling. *Acta Mater. Transylvanica* **2023**, *6*, 23–28.
18. Seleznev, A.; Pinargote, N.W.S.; Smirnov, A. Ceramic Cutting Materials and Tools Suitable for Machining High-Temperature Nickel-Based Alloys: A Review. *Metals* **2021**, *11*, 1385. [CrossRef]
19. Jacso, A.; Szalay, T.; Sikarwar, B.S.; Phanden, R.K.; Singh, R.K.; Ramkumar, J. Investigation of conventional and ANN-based feed rate scheduling methods in trochoidal milling with cutting force and acceleration constraints. *Int. J. Adv. Manuf. Technol.* **2023**, *127*, 487–506. [CrossRef]
20. Jacso, A.; Sikarwar, B.S.; Phanden, R.K.; Singh, R.K.; Ramkumar, J.; Sahu, G.N. Optimisation of tool path shape in trochoidal milling using B-spline curves. *Int. J. Adv. Manuf. Technol.* **2022**, *121*, 3801–3816. [CrossRef]
21. Líska, J.; Kun, K.; Kovács, Z. Attendants at MMC Composite Milling. In *Advances in Manufacturing Engineering and Materials II*; Hloch, S., Klichová, D., Pude, F., Krolczyk, G.M., Chattopadhyaya, S., Eds.; Springer International Publishing: Cham, Switzerland, 2021; pp. 332–342.
22. Monaca, A.; Axinte, D.A.; Liao, Z.; M'Saoubi, R.; Hardy, M.C. Towards understanding the thermal history of microstructural surface deformation when cutting a next generation powder metallurgy nickel-base superalloy. *Int. J. Mach. Tools Manuf.* **2021**, *168*, 103765. [CrossRef]
23. Móricz, L.; János, Z.V. Investigation of ductile/brittle chip formation zone in the context of manufactured geometry with different CAM paths strategies. *IFAC-PapersOnLine* **2022**, *55*, 2300–2305.
24. Patel, T.; Khanna, N.; Yadav, S.; Shah, P.; Sarikaya, M.; Singh, D.; Gupta, M.K. Machinability analysis of nickel-based superalloy Nimonic 90: A comparison between wet and LCO2 as a cryogenic coolant. *Int. J. Adv. Manuf. Technol.* **2021**, *113*, 3613–3628. [CrossRef]
25. Guo, C.; Chen, X.; Li, Q.; Ding, G.; Yue, H.; Zhang, J. Milling optimization of GH4169 nickel–based superalloy under minimal quantity lubrication condition based on multi-objective particle swarm optimization algorithm. *Int. J. Adv. Manuf. Technol.* **2022**, *123*, 3983–3994. [CrossRef]
26. Korkmaz, M.E.; Gupta, M.K.; Boy, M.; Yaşar, N.; Krolczyk, G.M.; Günay, M. Influence of duplex jets MQL and nano-MQL cooling system on machining performance of Nimonic 80A. *J. Manuf. Process.* **2021**, *69*, 112–124. [CrossRef]

27. Pereira, O.; Celaya, A.; Urbikaín, G.; Rodríguez, A.; Fernández-Valdivielso, A.; de Lacalle, L.N.L. CO_2 cryogenic milling of Inconel 718: Cutting forces and tool wear. *J. Mater. Res. Technol.* **2020**, *9*, 8459–8468. [CrossRef]
28. Wang, F.; Wang, Y. Comparison of cryogenic cooling strategy effects on machinability of milling nickel-based alloy. *J. Manuf. Process.* **2021**, *66*, 623–635. [CrossRef]
29. Villarrazo, N.; Caneda, S.; Pereira, O.; Rodríguez, A.; de Lacalle, L.N.L. The Effects of Lubricooling Ecosustainable Techniques on Tool Wear in Carbon Steel Milling. *Materials* **2023**, *16*, 2936. [CrossRef]
30. Wu, X.; Zhu, W.; Chen, J. Tool wear mechanisms in laser-assisted milling of Nickel-based superalloys. *J. Braz. Soc. Mech. Sci. Eng.* **2021**, *43*, 151. [CrossRef]
31. Zhang, H.; Yan, R.; Deng, B.; Lin, J.; Yang, M.; Peng, F. Investigation on surface integrity in laser-assisted machining of Inconel 718 based on in-situ observation. *Procedia CIRP* **2022**, *108*, 129–134. [CrossRef]
32. Parida, A.K.; Maity, K. Experimental investigation on tool life and chip morphology in hot machining of Monel-400. *Eng. Sci. Technol. Int. J.* **2018**, *21*, 371–379. [CrossRef]
33. Parida, A.K.; Maity, K. Numerical and experimental analysis of specific cutting energy in hot turning of Inconel 718. *Measurement* **2018**, *133*, 361–369. [CrossRef]
34. Kim, E.J.; Lee, C.M. A Study on the Optimal Machining Parameters of the Induction Assisted Milling with Inconel 718. *Materials* **2019**, *12*, 233. [CrossRef] [PubMed]
35. Baili, M.; Wagner, V.; Dessein, G.; Sallaberry, J.; Lallement, D. An Experimental Investigation of Hot Machining with Induction to Improve Ti-5553 Machinability. *Appl. Mech. Mater.* **2011**, *62*, 67–76. [CrossRef]
36. Gupta, M.K.; Niesłony, P.; Korkmaz, M.E.; Kuntoğlu, M.; Królczyk, G.M.; Günay, M.; Sarikaya, M. Comparison of Tool Wear, Surface Morphology, Specific Cutting Energy and Cutting Temperature in Machining of Titanium Alloys Under Hybrid and Green Cooling Strategies. *Int. J. Precis. Eng. Manuf.-Green Technol.* **2023**, *10*, 1393–1406. [CrossRef]
37. Kovács, Z.F.; Viharos, Z.J.; Kodácsy, J. Improvements of surface tribological properties by magnetic assisted ball burnishing. *Surf. Coat. Technol.* **2022**, *437*, 128317. [CrossRef]
38. Pimenov, D.Y.; da Silva, L.R.R.; Machado, A.R.; França, P.H.P.; Pintaude, G.; Unune, D.R.; Kuntoğlu, M.; Krolczyk, G.M. A comprehensive review of machinability of difficult-to-machine alloys with advanced lubricating and cooling techniques. *Tribol. Int.* **2024**, *196*, 109677. [CrossRef]
39. Liao, Y.S.; Lin, H.M. Mechanism of minimum quantity lubrication in high-speed milling of hardened steel. *Int. J. Mach. Tools Manuf.* **2007**, *47*, 1660–1666. [CrossRef]
40. Li, M.; Yu, T.; Yang, L.; Li, H.; Zhang, R.; Wang, W. Parameter optimization during minimum quantity lubrication milling of TC4 alloy with graphene-dispersed vegetable-oil-based cutting fluid. *J. Clean. Prod.* **2019**, *209*, 1508–1522. [CrossRef]
41. Karmiris-Obratanski, P.; Karkalos, N.E.; Kudelski, R.; Markopoulos, A.P. Experimental study on the effect of the cooling method on surface topography and workpiece integrity during trochoidal end milling of Incoloy 800. *Tribol. Int.* **2022**, *176*, 107899. [CrossRef]
42. Singh, R.; Sharma, V. Machining induced surface integrity behavior of nickel-based superalloy: Effect of lubricating environments. *J. Mater. Process. Technol.* **2022**, *307*, 117701. [CrossRef]
43. Sharma, A.K.; Singh, R.K.; Dixit, A.M.; Tiwari, A.K. Characterization and experimental investigation of Al_2O_3 nanoparticle based cutting fluid in turning of AISI 1040 steel under minimum quantity lubrication (MQL). *Mater. Today Proc.* **2016**, *3*, 1899–1906.
44. Said, Z.; Gupta, M.; Hegab, H.; Arora, N.; Khan, A.M.; Jamil, M.; Bellos, E. A comprehensive review on minimum quantity lubrication (MQL) in machining processes using nano-cutting fluids. *Int. J. Adv. Manuf. Technol.* **2019**, *105*, 2057–2086. [CrossRef]
45. Wang, C.; Li, K.; Chen, M.; Liu, Z. Evaluation of minimum quantity lubrication effects by cutting force signals in face milling of Inconel 182 overlays. *J. Clean. Prod.* **2015**, *108*, 145–157. [CrossRef]
46. Çakīr, O.; Yardimeden, A.; Ozben, T.; Kilickap, E. Selection of cutting fluids in machining processes. *J. Achiev. Mater. Manuf. Eng.* **2007**, *25*, 99–102.
47. Adler, D.; Hii, W.-S.; Michalek, D.; Sutherland, J. Examining the role of cutting fluids in machining and efforts to address associated environmental/health concerns. *Mach. Sci. Technol.* **2006**, *10*, 23–58. [CrossRef]
48. Khanna, N.; Shah, P.; Chetan. Comparative analysis of dry, flood, MQL and cryogenic CO_2 techniques during the machining of 15-5-PH SS alloy. *Tribol. Int.* **2020**, *146*, 106196.
49. Peralta Álvarez, M.E.; Marcos Bárcena, M.; Aguayo González, F. On the sustainability of machining processes. Proposal for a unified framework through the triple bottom-line from an understanding review. *J. Clean. Prod.* **2017**, *142*, 3890–3904. [CrossRef]
50. Lawal, S.; Choudhury, I.; Nukman, Y. Application of vegetable oil-based metalworking fluids in machining ferrous metals—A review. *Int. J. Mach. Tools Manuf.* **2012**, *52*, 1–12. [CrossRef]
51. Xu, X.; Huang, S.; Wang, M.; Yao, W. A study on process parameters in end milling of AISI-304 stainless steel under electrostatic minimum quantity lubrication conditions. *Int. J. Adv. Manuf. Technol.* **2017**, *90*, 979–989. [CrossRef]
52. Gajrani, K.K.; Suvin, P.S.; Kailas, S.V.; Sankar, M.R. Hard machining performance of indigenously developed green cutting fluid using flood cooling and minimum quantity cutting fluid. *J. Clean. Prod.* **2019**, *206*, 108–123. [CrossRef]
53. Hadad, M.; Hadi, M. An investigation on surface grinding of hardened stainless steel S34700 and aluminum alloy AA6061 using minimum quantity of lubrication (MQL) technique. *Int. J. Adv. Manuf. Technol.* **2013**, *68*, 2145–2158. [CrossRef]
54. Debnath, S.; Reddy, M.M.; Yi, Q.S. Environmental friendly cutting fluids and cooling techniques in machining: A review. *J. Clean. Prod.* **2014**, *83*, 33–47. [CrossRef]

55. Sen, B.; Mia, M.; Krolczyk, G.; Mandal, U.K.; Mondal, S.P. Eco-friendly cutting fluids in minimum quantity lubrication assisted machining: A review on the perception of sustainable manufacturing. *Int. J. Precis. Eng. Manuf.-Green Technol.* **2021**, *8*, 249–280. [CrossRef]
56. Singh, T.; Singh, P.; Dureja, J.S.; Dogra, M.; Singh, H.; Bhatti, M.S. A review of near dry machining/minimum quantity lubrication machining of difficult to machine alloys. *Int. J. Mach. Mach. Mater.* **2016**, *18*, 213. [CrossRef]
57. da Silva, L.R.R.; Ruzzi, R.S.; Teles, V.C.; Sales, W.F.; Guesser, W.L.; Machado, A.R. Analysis of the coefficient of friction at the workpiece-tool interface in milling of high strength compacted graphite cast irons. *Wear* **2019**, *426–427*, 1646–1657. [CrossRef]
58. Behera, B.C.; Alemayehu, H.; Ghosh, S.; Rao, P.V. A comparative study of recent lubri-coolant strategies for turning of Ni-based superalloy. *J. Manuf. Process.* **2017**, *30*, 541–552. [CrossRef]
59. Kaynak, Y.; Gharibi, A.; Yılmaz, U.; Köklü, U.; Aslantaş, K. A comparison of flood cooling, minimum quantity lubrication and high pressure coolant on machining and surface integrity of titanium Ti-5553 alloy. *J. Manuf. Process.* **2018**, *34*, 503–512. [CrossRef]
60. Kónya, G.; Kovács, Z.F. Experimental investigation of the effects of cooling-lubricating methods on the slot milling process of GTD-111 type nickel-based superalloy. *J. Manuf. Process.* **2024**, *119*, 98–108. [CrossRef]
61. Bao, X.; Yao, P.; Xu, J.; Mei, Z.; Li, Y.; Yang, J.; Wang, Q.; Chen, Z.; Qu, S. Effect of tool geometry and cutting parameters on surface quality and chip morphology of amorphous electroless nickel-phosphorus alloy in ultra-precision turning. *Int. J. Adv. Manuf. Technol.* **2023**, *126*, 2461–2478. [CrossRef]
62. Peta, K.; Bartkowiak, T.; Rybicki, M.; Galek, P.; Mendak, M.; Wieczorowski, M.; Brown, C.A. Scale-dependent wetting behavior of bioinspired lubricants on electrical discharge machined Ti6Al4V surfaces. *Tribol. Int.* **2024**, *194*, 109562. [CrossRef]